Research on the Molecular Entanglement and Disentanglement in the Dry Spinning Process of UHMWPE/Decalin Solution

Yushan Sun,[1,2] Yourong Duan,[1,3] Xueying Chen,[1] Qi Zhang,[2] Xiaofang Jin,[2] Xiaojun Li,[2] Yan Ma,[2] Lin Sun,[1] Qingrei Wang[1]

[1]*College of Materials Science and Engineering, Donghua University, Shanghai 200051, People's Republic of China*
[2]*Research and Development Center, China Textile Academy, Beijing 100025, People's Republic of China*
[3]*Shanghai Cancer Institute, Shanghai Jiao Tong University, Shanghai 200032, People's Republic of China*

Received 25 June 2005; accepted 18 October 2005
DOI 10.1002/app.23672
Published online in Wiley InterScience (www.interscience.wiley.com).

ABSTRACT: The macromolecular entanglement and disentanglement in the dry spinning process of ultrahigh molecular weight polyethylene (UHMWPE)/decalin solution were investigated. By the fitting results of the theoretical model to the experimental data, it is found that the variation tendency of the N_skT value, which reflects the chain slippage at the slip links in the extensional deformation on spinning line of draw-down process, is in accordance with the fact that each of the relationship curves between the tensile strength, modulus of the UHMWPE fibers through maximized solid state drawing and the draw-down ratio showed a peak, thus discovering the molecular movement mechanism of "disentanglement on spinning line." When the entanglements were included in the flow units, their apparent quantity would decrease. Based on this result, the optimum draw-down ratio can be determined directly by measuring the draw-down stress at the exit of the spinning duct. The molecular entanglements numbers, which are derived from the theoretical fitting to the experimental data of predrawing and after-drawing process, abruptly increased in large amounts. It may be concluded that these are mainly not attributed to the topological entanglements, but attributed to the agglomerate entanglements. © 2006 Wiley Periodicals, Inc. J Appl Polym Sci 102: 864–875, 2006

Key words: high performance polyethylene fiber; macromolecular entanglement; extrusion; drawing; structure–property relations

INTRODUCTION

In recent years, some methods on the control of draw-down process in the multihole gel spinning (wet spinning)[1] and dry spinning[2] of the ultrahigh molecular weight polyethylene (UHMWPE) solution have been patent. In our pervious report,[3] the relationship between the draw-down ratio in the dry spinning process of the UHMWPE/decalin solution and the fiber performance (tensile strength, modulus) through maximized solid state drawing was investigated. An optimum draw-down ratio (a peak value for each of the fiber performance and draw-down ratio relationship curves) could be found in the multihole dry spinning process, which was explained qualitatively by molecular disentanglement on spinning line during draw-down. In this article, the molecular entanglements were quantitatively analyzed based on the experimental data and the theoretical model of two components (entropy and viscosity) presented in our previous article.[3] The results of "peak phenomenon" are discussed by molecular movement mechanism.

Correspondence to: Y. Duan (duanyourong@hotmail.com).

Journal of Applied Polymer Science, Vol. 102, 864–875 (2006)

EXPERIMENTAL

The process of the dry spinning of the UHMWPE/decalin solution and the solid state drawing of the as-spun filaments (obtained by draw-down of the spinning dope and subsequent solvent evaporation) were basically the same as described in detail in our pervious report.[3] The suspension slurry of 6% w/v (PE weight/decalin volume) of UHMWPE nascent powder (a commercial product PE M-IV from Beijing Auxiliaries Plant No. 2, Beijing, China) and antioxidant was fed to a corotating twin-screw extruder for dissolving and deaeration. The spinning dope from the twin-screw extruder went through the booster pump, the static mixer, the prefilter, to the spinning trunk, and then it was pumped through a 364-hole spinneret of 0.6 mm diameter. The spinning temperature was 190°C and the extrusion speed was 1.88 m/min. When the extruded thread line went out of the spinning line oven (37 cm in length) after draw-down, it was immediately blown by cross N_2 gas (at 80°C) flow coming from a lateral blow window screen; then it went through an 8-m high vertical duct with gas (at 115–80°C) flowing from the lower part to the upper part. The dry as-spun filaments from the exit of the spinning duct were drawn in solid state by con-

tinuous predrawing in the fore-spinning section and multistage drawing in separate after-drawing section.

The extensional force (tensile force) in the draw-down process was measured at the exit of the spinning duct by DTMB-1000 tension meter (made by HANS SCHMIDT and Co GmbH, Waldkraiburg, Germany); the extensional force of the predrawing in the fore-spinning section and the extensional forces of the multistage drawing in the after-drawing section were measured by DTMB-10K tension meter.

The thermal shrinkage (melting shrinkage exactly) was determined using a capillary tube in silicone oil with controlled temperature.[4] The monofilament sample was guided into a ϕ0.5 mm $\times$ 200 mm capillary tube by a copper wire and then the silicone oil was injected. After that, the capillary tube was vertically immersed in the silicone oil bath, and the length of monofilament in the silicone oil bath was 180 mm. The silicone oil bath was heated up from room temperature to 142°C, and then after 20 min, the capillary tube was taken out of the bath. The monofilament was taken out and the length after its shrinkage was measured. The thermal shrinkage was determined by $\Delta L/L$, where ΔL is the difference of the length before and after the thermal shrinkage; L is the length before the thermal shrinkage.

The unconstrained and constrained DSC thermograms were measured by using a PerkinElmer Pyris 1 DSC differential scanning calorimeter at a heating rate of 5°C/min in a nitrogen atmosphere. Indium standard was used for temperature calibration. An empty sample pan was taken as the reference sample. The fiber samples were cut into pieces of 2–3 mm in length, or wound round an aluminum plate, respectively, for unconstrained or constrained measurements. Scans were conducted from 60 to 180°C. The crystallinity was calculated by $\Delta H/\Delta H^0$, taking the heat of fusion ΔH^0 for perfect crystalline polyethylene as 292.8 kJ/kg.[4]

The viscosity average molecular weight $\overline{M}_v$ was determined with reference to ASTM D 4020−01a standard.[5] The UHMWPE nascent powder was dissolved in decalin containing 0.2% antioxidant at 150°C for 1 h, and then after 30 min of equilibrium time at (135 ± 0.1)°C in an Ubbeledhe viscometer (capillary diameter 0.55 mm), the flow time was measured. For the UHMWPE fiber sample, the fiber was cut into pieces, after cut, it was swollen at 95°C for 3 h, and then dissolved in decalin containing 0.2% antioxidant at 160°C for 1 h. After 30 min of equilibrium time at (135 ± 0.1)°C in the Ubbeledhe viscometer, the flow time was measured. The viscosity average molecular weight $\overline{M}_v$ was calculated from the following equations[5]:

$$\eta_r=(t-D/t)/(t_0-D/t_0) \tag{1}$$

$$\eta_{sp}=\eta_r-1 \tag{2}$$

$$[\eta]=[2(\eta_{sp}-\ln\eta_r)]^{0.5}/C \tag{3}$$

$$\overline{M}_v = 5.37\times10^4[\eta]^{1.37} \tag{4}$$

where η_r is the relative viscosity; t_0 and t(s) are the flow time of the solvent and solution, respectively; D is the correction factor of the viscometer (s^2); η_{sp} is the specific viscosity; $[\eta]$ is the intrinsic viscosity(dl/g); C is the polymer concentration (g/dL).

RESULTS AND DISCUSSION

Free energy calculation equation for the developed macromolecular entanglements model is as follows[6–9]:

$$F=\frac{1}{2}N_ckT\left[\frac{\sum(1-\alpha^2)\lambda_i^2}{1-\alpha^2\lambda_i^2}+\ln(1-\alpha^2\sum\lambda_i^2)\right]+\frac{1}{2}N_skT\left\{\sum\left[\frac{\lambda_i^2(1+\beta)(1-\alpha^2)}{(1+\beta\lambda_i^2)(1-\alpha^2\sum\lambda_i^2)}+\ln(1+\beta\lambda_i^2)\right]+\ln(1-\alpha^2\sum\lambda_i^2)\right\} \tag{5}$$

where N_c represents the network chain number of the fixed molecular chain entanglements (highly tangled and equivalently crosslinked); N_s is the network chain number of the slip entanglements; λ, the draw ratio; k, the Boltzmann constant; T, the absolute temperature; α, a measure of the inextensibility; β is a measure of the freedom of a link to slide compared with the freedom of movement of a chain. Supposing the extensional deformation by draw-down basically occurred before solvent evaporation in the dry spinning process of the UHMWPE/decalin solution and in the uniaxial drawing:

$$\lambda_1=\lambda;\ \lambda_2=\lambda_3=\lambda^{-1/2} \tag{6}$$

The entropic force σ_e can be calculated by[7,9]

$$\sigma_e=\left(\frac{\partial F}{\partial\lambda}\right)_{TV}=N_ckT\frac{D}{1-\alpha^2\phi}\left(\frac{1-\alpha^2}{1-\alpha^2\phi}-\alpha^2\right)+N_skT\left\{\frac{(1-\alpha^2)(1+\beta)}{1-\alpha^2\phi}\left[\frac{\alpha^2D}{1-\alpha^2\phi}\left(\frac{\lambda^2}{1+\beta\lambda^2}+\frac{2}{\lambda+\beta}\right)+\frac{\lambda}{(1+\beta\lambda^2)^2}-\frac{1}{(\lambda+\beta)^2}\right]+\beta\left[\frac{\lambda}{1+\beta\lambda^2}-\frac{1}{\lambda(\lambda+\beta)}\right]-\frac{\alpha^2D}{1-\alpha^2\phi}\right\} \tag{7}$$

where ϕ and D are given by

$$\phi=\lambda^2+\frac{2}{\lambda};\ D=\frac{1}{2}\frac{d\phi}{d\lambda}=\lambda-\frac{1}{\lambda^2} \tag{8}$$

TABLE I
The Experimental Data of Tensile Stress for Different Draw-Down Ratio

Draw-down ratio λ_{ext}	2.128	3.191	4.255	5.319	6.383	7.447	8.511	9.574	10.638
Tensile stress (kPa)	13.69	22.43	23.98	25.24	27.38	29.71	35.24	38.83	48.25

V_0 = 1.88 m/min; L = 0.37 m.

Other parameters have the same meanings as mentioned earlier. Besides the entropic force σ_e, in practical process the relative movement of the macromolecular chains would be hindered by the viscous force (internal friction force). According to the two components model of entropy component and viscosity component, presented in our previous article,[3] where the Hooke spring of Voight viscoelastic model was replaced by an "entropy spring " based on the developed macromolecular entanglements model, the drawing stress can be expressed as

$$\sigma = \sigma_v + \sigma_e \tag{9}$$

where σ_e is given by eq. (7) and σ_v is given by

$$\sigma_v = \eta\dot{\varepsilon};\ \dot{\varepsilon} = V_0(\lambda - 1)/L \tag{10}$$

where $\dot{\varepsilon}$ is the drawing strain rate; V_0, the extrusion speed (or feeding speed of drawing); L, the length of the strain region; λ, the draw ratio (hereafter the draw ratio λ is noted as λ_{ext} in the extrusion process, λ_{pre} in the predrawing process, λ_{adr1} in the first step afterdrawing process, and λ_{adr2} in the second step afterdrawing process); η represents the extensional viscosity (not including the elastic content, which has been attributed to the molecular entanglements and entropy variation) reflecting the viscous or internal friction extent between chain segments of relative movement, which is related to the intermolecular distance and the movement unit length of the macromolecular chains. The entropy–viscosity model sets up the relationship between the macroscopic measurable quantity (drawing stress) and the microcosmic quantity (macromolecular entanglements).

The experimental results of the tensile stress (extensional stress) σ versus the draw-down ratio λ_{ext} with fixed extrusion speed (1.88 m/min) are shown in Table I. The nine experimental points were separated into five groups: 1–5; 2–6; 3–7; 4–8; 5–9 points for the first to the fifth group, respectively. For instance, the 1–5 points (see Table I) for the first group are (draw-down ratio λ, tensile stress σ/kPa): (2.128, 13.69); (3.191, 22.43); (4.255, 23.98); (5.319, 25.24); (6.383, 27.38), and the 2–6 points for the second group are (3.191, 22.43); (4.255, 23.98); (5.319, 25.24); (6.383, 27.38); (7.447, 29.71), and so on. From eqs. (7)–(10), the relationship between draw ratio λ and drawing stress σ (draw-down ratio and tensile stress) is set up, in which the five parameters $\alpha^2\beta$, N_ckT, N_skT and η are to be determined by the experimental data of each group of the five groups. In the fitting and calculating process for each group, the value range of α^2 was from 0 to 1 and β from 0 to 2.[6–9] The value ranges of N_ckT, N_skT and η were determined by giving them initial ranges first and then readjusting them according to the calculating results. If the calculated value of N_ckT, N_skT or η is at the upper limit of the given value range, the value range should be extended the next time. For more accurate fitting result, the step length of calculation should be reduced. After the determination of the five parameters α,[2] β, N_ckT, N_skT, and η, the σ–λ relationship equation and its curve of the theoretical model was obtained. Figures 1–5 reflect the fitting results of the theoretical model [eqs. (7)–(10)] to the five groups of experimental data by computer using a calculating program of least squares criterion. Table II presents the fitted values of the parameters in the theoretical model for the five groups of experimental data. It needs to be pointed out that the average draw-down ratio $\bar{\lambda}$ and corresponding average extensional strain rate $\bar{\dot{\varepsilon}}$ in Figures 1–5 and Table II are used only to characterize each group of the five intentionally divided groups from the experimental data in Table I, not to calculate in the curve fitting. In each group, the five parameters α,[2] β, N_ckT, N_skT and η are presumed to be constant (in fact, they are also average values

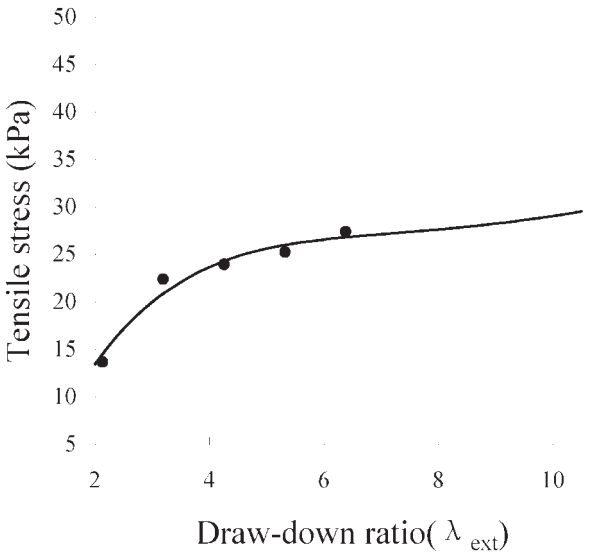

Figure 1 Tensile stress of the draw-down versus the draw-down ratio for $\bar{\dot{\varepsilon}}$ = 0.276 s^{-1}; (●) experimental; (−) theoretical.

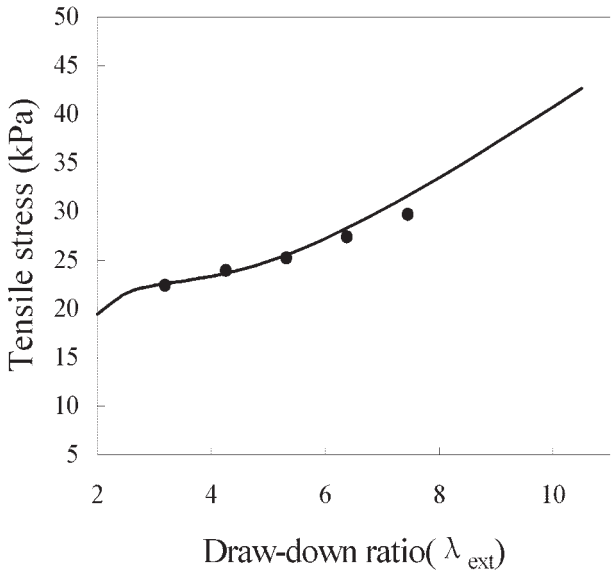

Figure 2 Tensile stress of the draw-down versus the draw-down ratio for $\bar{\dot{\varepsilon}} = 0.366\ s^{-1}$; (●) experimental; (−) theoretical.

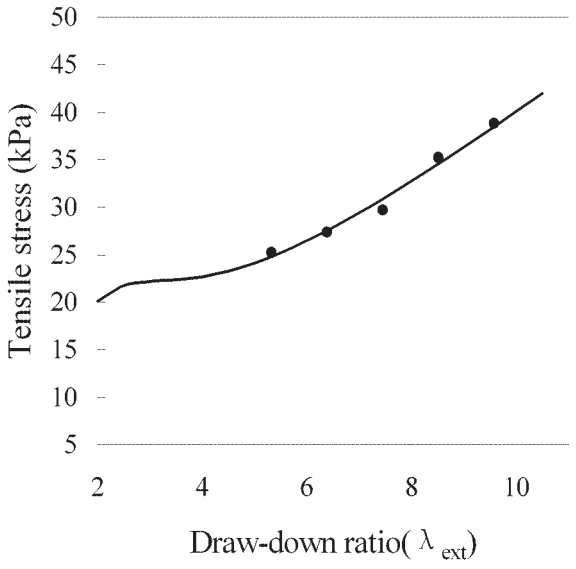

Figure 4 Tensile stress of the draw-down versus the draw-down ratio for $\bar{\dot{\varepsilon}} = 0.546\ s^{-1}$; (●) experimental; (−) theoretical.

corresponding to the $\bar{\lambda}$ or $\bar{\dot{\varepsilon}}$ range), and they are fitted out by the five (λ, σ) points of each group. From Table II, it can be seen that the inextensibility factor α^2 was equal to zero in the whole experimental range of the draw-down process. The slip link freedom factor β increased with the increase in $\bar{\lambda}$ and$\bar{\dot{\varepsilon}}$, then tended to be constant. The extensional viscosity η increased with the increase in $\bar{\lambda}$ and $\bar{\dot{\varepsilon}}$ in the whole range, which reflected the increase of the molecular chain movement unit amount or their lengths (the concentration and temperature of the spinning dope, which are related to the intermolecular distance, were the same for the five groups of experimental data). In the lower $\bar{\lambda}$ and $\bar{\dot{\varepsilon}}$ range, the N_ckT values (reflecting the fixed molecular chain entanglements) are higher and increase with the increase of $\bar{\lambda}$ and $\bar{\dot{\varepsilon}}$ (see Table II). This is because the η value (reflecting the viscous force or internal friction force) and extensional stress were both smaller in this range, and compared with the relatively easier molecular chain movement, even looser tangles would behave as fixed entanglements, which increased with the increase in $\bar{\lambda}$ and $\bar{\dot{\varepsilon}}$. When the $\bar{\lambda}$ and $\bar{\dot{\varepsilon}}$ continuously increased to a considerable level ($\bar{\lambda} = 6.38$, $\bar{\dot{\varepsilon}} = 0.456\ s^{-1}$), the extensional defor-

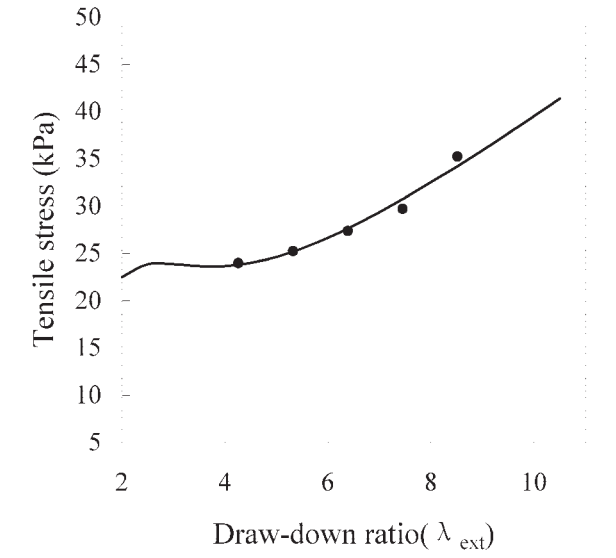

Figure 3 Tensile stress of the draw-down versus the draw-down ratio for $\bar{\dot{\varepsilon}} = 0.456\ s^{-1}$; (●) experimental; (−) theoretical.

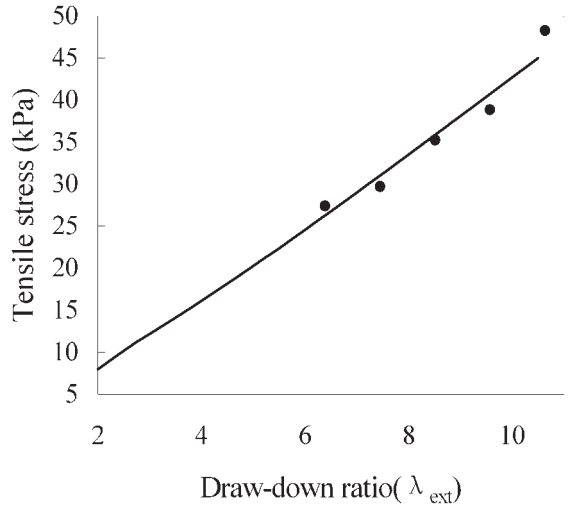

Figure 5 Tensile stress of the draw-down versus the draw-down ratio for $\bar{\dot{\varepsilon}} = 0.636\ s^{-1}$; (●) experimental; (−) theoretical.

TABLE II
The Fitted Parameters for the Molecular Entanglement Model of Entropy and Viscosity Composition for Different Draw-Down

Parameter	Parameter value				
	$\bar{\lambda}$=4.26; $\bar{\dot{\varepsilon}}$ = 0.276 s^{-1}	$\bar{\lambda}$=5.32; $\bar{\dot{\varepsilon}}$ = 0.366 s^{-1}	$\bar{\lambda}$ = 6.38; $\bar{\dot{\varepsilon}}$ = 0.456 s^{-1}	$\bar{\lambda}$ = 7.45; $\bar{\dot{\varepsilon}}$ = 0. 546 s^{-1}	$\bar{\lambda}$ = 8.51; $\bar{\dot{\varepsilon}}$ = 0.636 s^{-1}
α^2	0	0	0	0	0
β	0.02	0.12	0.15	0.14	0.15
N_ckT (kPa)	0.7	1.1	0.005	0.1	0.1
N_skT (kPa)	7	16	23	19	4
η (kPa s)	18	36	48	48	54

V_0 = 1.88 m/min; L = 0.37 m.

mation was mainly related to the slippage between molecular chains, and at this moment the N_ckT value was the lowest. With further increase in $\bar{\lambda}$ and $\bar{\dot{\varepsilon}}$, the originally looser tangles became tighter and behaved as fixed entanglements again. Thus, the N_ckT value increased once more. At this stage the N_ckT value virtually reflected the tight tangles, and its amount was smaller than that of looser tangles in the lower $\bar{\lambda}$ and $\bar{\dot{\varepsilon}}$ range. The N_skT value, which reflects the slip entanglements, showed the network chains number per unit volume, relative to the chain slippage at the macromolecular entanglement points during the extensional deformation. The higher N_skT value, the more probability of "disentanglement on spinning line" through chain slippage. In the low range of $\bar{\lambda}$ and $\bar{\dot{\varepsilon}}$, with the increase of $\bar{\lambda}$ and $\bar{\dot{\varepsilon}}$, the N_skT increased, indicating that the network chains were related to chain slippage increase. Therefore, the extent of "disentanglement on spinning line" increased. After the peak value of N_skT, the N_skT value decreased with further increase in $\bar{\lambda}$ and $\bar{\dot{\varepsilon}}$. The reason for this may be that the chain slippage became more difficult due to the increase of viscous force. On the other hand, at high strain rate the movement of chain segment could not catch up with the strain rate, thus causing the decrease in network chains number of chain slippage. When the entanglements were included in the flow units, i.e., the entanglements moved together with the relative molecular chains (as moving clusters), the apparent entanglements number N_s would decrease, indicating that the disentanglements number would decrease. The bigger or longer flow unit was composed of highly tangled unoriented molecular group or elongated molecular cluster. Under excessive $\bar{\lambda}$ and $\bar{\dot{\varepsilon}}$ condition of the draw-down, i.e., when the molecular chain movement could not catch up with the deformation rate, the local structural disorder would easily be caused, thus resulting in permanent structural defects. These defects would affect the successive drawability of the fiber in solid state, and make the performance of the end fiber (through maximized solid state drawing) decreased. Figure 6 shows the relationship between the N_skT value and the average draw-down ratio $\bar{\lambda}$. It can be found that a peak value of the N_skT appeared with the increase in $\bar{\lambda}$ and then with further increase in $\bar{\lambda}$ the N_skT value decreased. This variation tendency is in accordance with that of the relationship curves between the fiber performance (tenacity and modulus) and the draw-down ratio, which has been reported in our pervious article.[3] Thus, discovering the molecular mechanism of "disentanglement on spinning line." Based on this result, the optimum draw-down ratio can be determined directly by measuring the draw-down stress at the exit of the spinning duct.

As for the exact entanglements number, it has been reported that the average entanglements number for each macromolecular chain in the UHMWPE end fiber

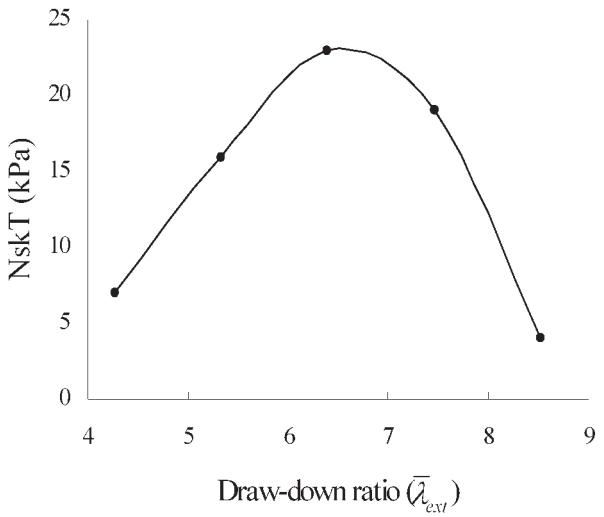

Figure 6 The slip link parameter N_skT of the chain entanglements versus the average draw-down ratio.

TABLE III
Viscosity Average Molecular Weight $\overline{M}_v$ of the Samples at Different Processing Stage

Sample	Nascent powder
$\overline{M}_v/10^4$	440

TABLE IV
The Results of Calculated Entanglement Number per Macromolecule in the UHMWPE End Fiber by Kalb-Smook Method[4,10]

Sample	$\overline{M}_v/10^4$	$\Delta L/L$	i
Experimental series 1	192	0.9333	6.21
Experimental series 2	192	0.9458	5.28

could be estimated by the thermal shrinkage measurement, as in the following equations[4,10]

$$\lambda_{\max} = L_0/2R_g = M^{1/2}/20.8 \tag{11}$$

$$\Delta L/L = (L_1 - 2R_g)/L_1 \tag{12}$$

where $\lambda_{\max}$ is the theoretically maximal draw ratio; L_0, the contour length of fully extended macromolecular chain; R_g, is the radius of gyration of fully relaxed macromolecule in the melt; M, the molecular weight; $\Delta L/L$, the practical thermal shrinkage rate; and L_1 is the practical length of the macromolecular chain after maximized hot drawing, we get

$$\frac{L_1}{L_0} = 20.8M^{-1/2}\left(1 - \frac{\Delta L}{L}\right)^{-1} \tag{13}$$

The average entanglements number for each macromolecular chain in fully drawn fiber can be estimated by the following equation[4]:

$$\frac{L_1}{L_0} = 0.8^{\mathrm{i}} \tag{14}$$

where L_1/L_0 can be calculated from eq. (13); i represents the entanglements number. It has been reported that when the weight average molecular weight $\overline{M}_w$ was adopted as M in calculation, it seemed to be slightly higher; when the number average molecular weight $\overline{M}_n$ was adopted as M in calculation, it seemed to be much lower.[10] In this study, the viscosity average molecular weight $\overline{M}_v$ was adopted as M in calculation. Table III presents the measured viscosity average molecular weight $\overline{M}_v$ of the samples in different processing stage. Although the dissolving conditions for nascent powder and fiber samples were somewhat different (considering the difficulty of dissolving fiber sample), it was found in the experimental range that the higher temperature only slightly affected the test results for nascent powder sample, so the test value for fiber sample can be considered to be closed to the true value (the antioxidant was about nine times the quantity of the UHMWPE powder according to ASTM D 4020–01a standard, so the degradation was effectively restrained). Table IV shows the results of calculated entanglements number per macromolecule. In Table IV, the experimental series 1 and experimental series 2 were respectively, corresponding to the feeding speeds 4 m/min and 2 m/min in after-drawing process, and other conditions for them were the same. Considering that the maximum draw ratio has practically been reduced to maintain steady and continuous operation of the after-drawing, the L_1/L_0 value was divided by a coefficient 0.9 for the calculation of entanglements number i. It can be seen from Table IV that the entanglements number of the end fiber sample of the experimental series 2 ($i = 5.28$, corresponding to the lower feeding speed and higher after-drawing ratio) was less than that of the experimental series 1 ($i = 6.21$), which indicated that the drawing condition in solid state would affect the entanglements number calculated by this method. As to the entanglements number of the draw-down process, when, for instance

$$N_s kT = 7 \text{ kPa} = 7 \times 10^3 \text{ N m}^{-2}$$

the network chains number N_s per unit volume can be calculated as

$$N_s = \frac{7 \times 10^3 \text{ N m}^{-2}}{1.3807 \times 10^{-23}\text{N m K}^{-1} \times (273.15 + 190)K} = 1.095 \times 10^{24} \text{ m}^{-3}$$

Take the density of the UHMWPE/decalin solution as $\rho = 0.88$ g cm^{-3}; the molecular weight $M = \overline{M}_v = 215 \times 10^4$ (see Table III), the mole number of the macromolecules per unit volume is given by

$$\frac{880 \text{ kg m}^{-3}}{2150 \text{ kg mol}^{-1}} = 0.409 \text{ mol m}^{-3}$$

TABLE V
The Shown Entanglement Number per Macromolecule and the Repeat Unit Number Between the Entanglements During the Draw-Down Process, Calculated from the Fitted Parameters of the Molecular Entanglement Model of Entropy and Viscosity Composition

N_cKt (kPa)	0.7	1.1	0.005	0.1	0.1
Equivalently fixed links	0.44	0.70	0.004	0.06	0.06
N_skT (kPa)	7	16	23	19	4
Slip links	4.45	10.14	14.58	12.06	2.54
—CH_2— number between the entanglements/10^4	3.14	1.42	1.06	1.28	5.9

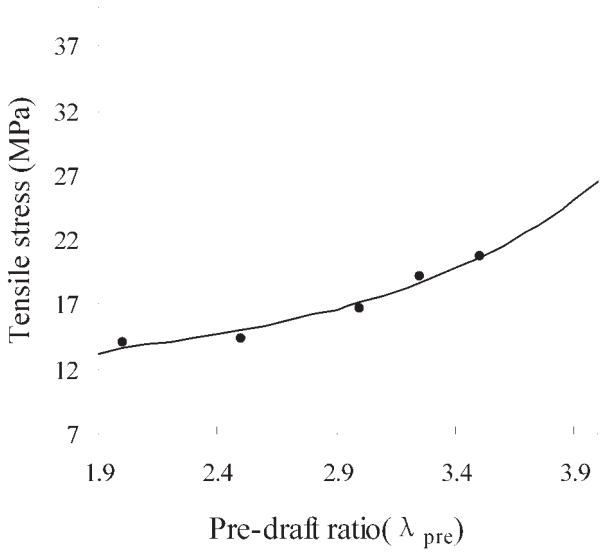

Figure 7 Tensile stress of the predraft versus the predraft ratio for $\bar{\dot{\varepsilon}} = 0.077\ s^{-1}$; (●) experimental; (−) theoretical.

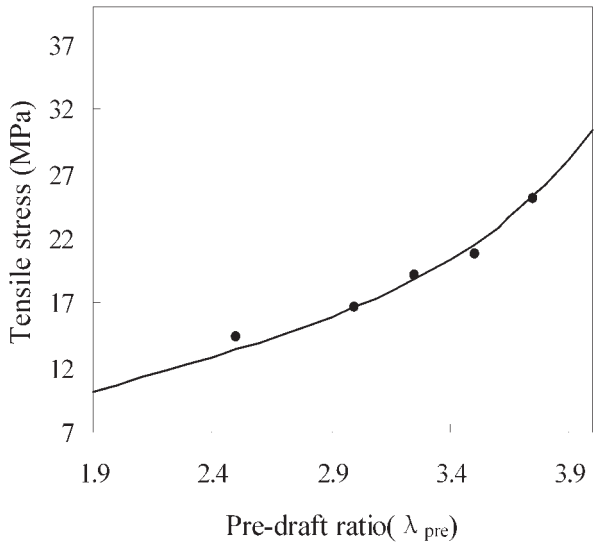

Figure 8 Tensile stress of the predraft versus the predraft ratio for $\bar{\dot{\varepsilon}} = 0.092\ s^{-1}$; (●) experimental; (−) theoretical.

The macromolecules number per unit volume is given by $0.409N_A$ (Avogadro constant) = 0.409 mol m^{-3} × 6.022 × 10^{23} mol^{-1} = 2.463 × 10^{23} m^{-3}.

The average slip entanglements number per macromolecule is equal to the network chains number per unit volume/the macromolecules number per unit volume.

$$\frac{1.095 \times 10^{24}\ m^{-3}}{2.463 \times 10^{23}\ m^{-3}} = 4.45$$

The entanglements number of the draw-down process calculated from the N_skT and N_ckT values of Table II are shown in Table V. For the repeat unit —CH_2— number between entanglements in Table V, when, for example, N_skT = 7 kPa; N_ckT = 0.7 kPa, the repeat unit —CH_2— number per macromolecule is given by

$$M/M_{CH_2} = 215 \times 10^4/14 = 15.36 \times 10^4$$

The repeat unit —CH_2— number between entanglements is given by the repeat unit —CH_2— number per macromolecule/network chains number per macromolecule.

$$\frac{15.36 \times 10^4}{4.45 + 0.44} = 3.14 \times 10^4$$

From Table V, it can be seen that the equivalently fixed links are very little, and the variation tendency of the repeat unit —CH_2— number between entanglements basically correspond to that of slip links. With the initial increase and later decrease of the slip links, the repeat unit —CH_2— number between entanglements correspondingly decreases firstly and increases afterwards.

For the predrawing process, the tensile stresses were measured by changing the running speed of the seven-roller machine after the hot draw box, while the speed before the hot draw box was fixed. Seven experimental points were separated into three groups and they were fitted by the theoretical model in the same way as mentioned above in the draw-down process. Figures 7–9 show the fitting results. Table VI presents the fitted values of the parameters in the theoretical model for the three groups of experimental data, where each group is represented by the average predraft ratio $\bar{\lambda}$ and average extensional strain rate $\bar{\dot{\varepsilon}}$.

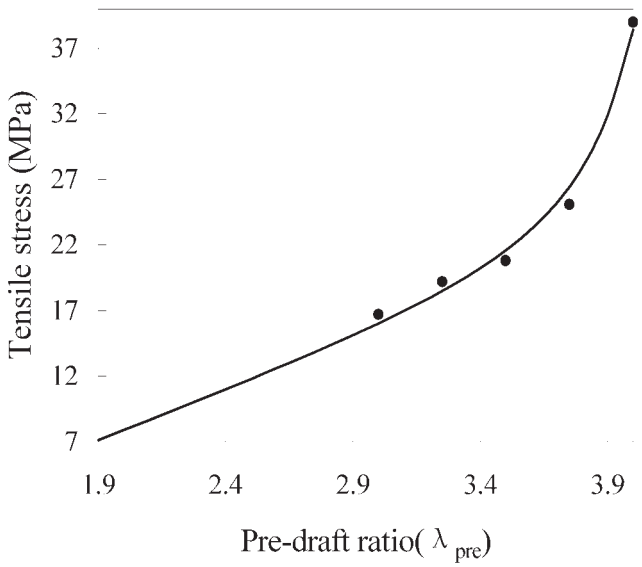

Figure 9 Tensile stress of the predraft versus the predraft ratio for $\bar{\dot{\varepsilon}} = 0.104\ s^{-1}$; (●) experimental; (−) theoretical.

TABLE VI
The Fitted Parameters for the Molecular Entanglement Model of Entropy and Viscosity Composition for Different Predrawing

Parameter	Parameter value		
	$\bar{\lambda} = 2.85$; $\bar{\dot{\varepsilon}} = 0.077\ s^{-1}$	$\bar{\lambda} = 3.20$; $\bar{\dot{\varepsilon}} = 0.092\ s^{-1}$	$\bar{\lambda} = 3.5$; $\bar{\dot{\varepsilon}} = 0.\ 104\ s^{-1}$
α^2	0.02	0.03	0.05
β	0.52	0.23	0.25
$N_c kT$ (MPa)	1.1	0	0
$N_s kT$ (MPa)	27	8.6	0.6
η (MPa s)	0.36	78	174

$V_0 = 10$ m/min, $L = 4$ m.

For the entanglements number of predrawing process, when, for instance

$$N_s kT = 27\ \text{MPa} = 27 \times 10^6\ \text{N m}^{-2}$$

the network chains number N_s per unit volume can be calculated as

$$N_s = \frac{27 \times 10^6\ \text{N m}^{-2}}{1.3807 \times 10^{-23}\ \text{N m K}^{-1} \times (273.15 + 115)\text{K}} = 5.038 \times 10^{22}\ \text{m}^{-3}$$

According to the linear additive property, the specific volume of the fiber is given by

$$\frac{1}{\rho} = \frac{1}{\rho_c} \times c + \frac{1}{\rho_a} \times (1 - c) \qquad (15)$$

where ρ represents the fiber density; c is the crystallinity; ρ_c and ρ_a represent the densities of the crystalline and amorphous regions, taken as 1.00 and 0.85 g/cm^3, respectively.[11] It can be found from Table VII that the DSC crystallinity of the draw-down fiber sample ($\lambda = 1$, the fiber before the predrawing of the fore-spinning section) was 51.78%. Therefore, $\rho = 0.92$ derived from eq. (15). Take $M = \overline{M}_v = 215 \times 10^4$ (see Table III), the mole number of the macromolecules per unit volume is given by

$$\frac{920\ \text{kg m}^{-3}}{2150\ \text{kg mol}^{-1}} = 0.428\ \text{mol m}^{-3}$$

The macromolecules number per unit volume is given by:

$$0.428 N_A = 0.428\ \text{mol m}^{-3} \times 6.022 \times 10^{23}\ \text{mol}^{-1} = 2.577 \times 10^{23}\ \text{m}^{-3}$$

The average slip entanglement number per macromolecule is equal to

$$\frac{5.038 \times 10^{27}\ \text{m}^{-3}}{2.577 \times 10^{23}\ \text{m}^{-3}} = 19550$$

TABLE VIII
The Shown Entanglement Number per Macromolecule and the Repeat Unit Number Between the Entanglements During the Predrawing Process, Calculated from the Fitted Parameters of the Molecular Entanglement Model of Entropy and Viscosity Composition

$N_c kT$ (MPa)	1.1	0	0
Equivalently fixed links	796	0	0
$N_s kT$ (MPa)	27	8.6	0.6
Slip links	19550	6228	434
—CH_2— number between entanglements	7.55	24.65	354

The calculated entanglements number per macromolecule and the repeat unit —CH_2— number between entanglement for predrawing process are shown in Table VIII. It could be seen that the slip entanglement number of the predrawing process greatly increased when compared with that of the draw-down process. The abrupt increase in the entanglement number might be related to the agglomerate entanglements. The usual concept of the topological entanglements is that the macromolecule chains wind or knot each other, and cannot cut across between them. Therefore the molecular movement is restricted. Besides the topological entanglements, there is another kind of local agglomerate entanglements, which is caused by the cohesive effect of the local molecular chains.[12] Because of the anisotropy of Van der Waals force between molecular chains, the chain segments of two macromolecular chains tend to be locally parallelly arranged, thus forming entanglements. This phenomenon was also called the local orientation correlation or nematic interaction of the macromolecular chains. The local size of this kind of chain entanglements may be very little and it is not necessarily composed of two chains. One entanglement may be composed of several parallelly arranged chains. The density of agglomerate entanglements is much higher than that of topo-

TABLE VII
The Crystallinity Derived from DSC of the UHMWPE Fibers

Draw ratio in solid state	$\lambda = 1$	$\lambda = 4$	$\lambda = 15$	$\lambda = 19.61$	$\lambda = 23.1$
Crystallinity (%)	51.78	50.86	71.69	80.99	81.90

Experimental series 2.

TABLE IX
The First Melting Peak Temperatures in DSC of the UHMWPE Fibers

Sample	The first melting peak temperature (°C)				
	$\lambda = 1$	$\lambda = 4$	$\lambda = 10$	$\lambda = 16.5$	$\lambda = 17.5$
Fibers in unconstrained state	134.7	134.2	142.3	143.8	142.3
Fibers in constrained state	135.7	147.7	154.0	155.0	153.8

Experimental series 1.

logical entanglements.[12] This kind of entanglements mainly behaved as slip entanglements, and its density was easily affected by external conditions. From the research results of Raman spectroscopy and NMR, it was believed that the chain entanglements occurred in interfacial phase and noncrystalline phase. The interfacial phase contained both topological and agglomerate entanglements, but the noncrystalline region mainly contained topological entanglements.[13] From the high entanglement number (slip links: 19,550 etc.) and the low —CH_2— number between entanglements (7.5 etc.) in Table VIII, and the corresponding sample crystallinity (51.78%, see Table VII), it could be concluded that the molecular chains in the crystalline region have made contribution to the slip entanglements, i.e., the relative slippage of the molecular chains in the crystalline region and the crystalline rearrangement occurred, which behaved as slip or agglomerate entanglements. The shown slip entanglement number decreased rapidly with the increase of $\bar{\lambda}$ and $\dot{\bar{\varepsilon}}$, and the shown fixed entanglement number decreased quickly to zero. With the increase in $\bar{\lambda}$ and $\dot{\bar{\varepsilon}}$ in Table VI, the inextensibility factor α^2 increased slightly; the slippage freedom factor β decreased swiftly from higher value (0.52) to that of approaching theoretical value (0.2343)[9]; the extensional viscosity η promptly increased. As the drawing temperature was the same in the experimental series, the increase of η value should be related to the length of the molecular chain movement unit in the extensional deformation process.

Tables IX and X present the first melting peak temperatures in DSC of the UHMWPE fibers of the two experimental series. It was found that in this research, the optimum drawing temperature of different drawing step in the after-drawing process was basically in accordance with the first melting peak temperature in DSC of the fiber sample (before drawing) in unconstrained state.

Figures 10–13 show the fitting results of the theoretical model to the four groups of experimental data of the after-drawing process, where Figures 10 and 12 correspond to the first and second step after-drawing at 4 m/min of feeding speed (experimental series 1); Figures 11 and 13 correspond to the first and second step after-drawing at 2 m/min of feeding speed (experimental series 2). Table XI presents the fitted values of the parameters in the theoretical model for the four groups of experimental data of the after-drawing process, where $\bar{\lambda} = 2.51$ and $\bar{\lambda} = 1.39$ in the first and second step after-drawing correspond to the experimental series 1; $\bar{\lambda} = 3.4$ and $\bar{\lambda} = 1.31$ in the first and second step after-drawing correspond to the experimental series 2. It could be seen from Table XI that the inextensibility factor α^2 value was equal to zero for the first step after-drawing in both experimental series, but for the second step after-drawing, the α^2 was not equal to zero, and the α^2 value of the experimental series 2 (0.36) was smaller than that of the experimental series 1(0.41), which might be related to the low $\dot{\varepsilon}$ and $\bar{\lambda}$. The value of the slip link freedom factor β of the experimental series 2 (0.06) was higher than that of the experimental series 1 (0.03) for the first step after-drawing, which indicated that the lower feeding speed favored the chain slippage. For the second step after-drawing the β value of the experimental series 2 (0.46) was lower than that of the experimental series 1 (0.55). The reason for this might be that the first step after-drawing ratio of the experimental series 2 was higher. Therefore, the fiber structure was more compact before the second step after-drawing, which made the value of the slip link freedom factor β lower than the experimental series 1 in the second step after-drawing process. The N_ckT values of the four groups

TABLE X
The First Melting Peak Temperatures in DSC of the UHMWPE Fibers

Sample	The first melting peak temperature (°C)				
	$\lambda = 1$	$\lambda = 4$	$\lambda = 15$	$\lambda = 19.61$	$\lambda = 23.1$
Fibers in unconstrained state	134.7	134.2	140.6	142.2	143.6
Fibers in constrained state	135.7	147.7	152.9	153.7	154.3

Experimental series 2.

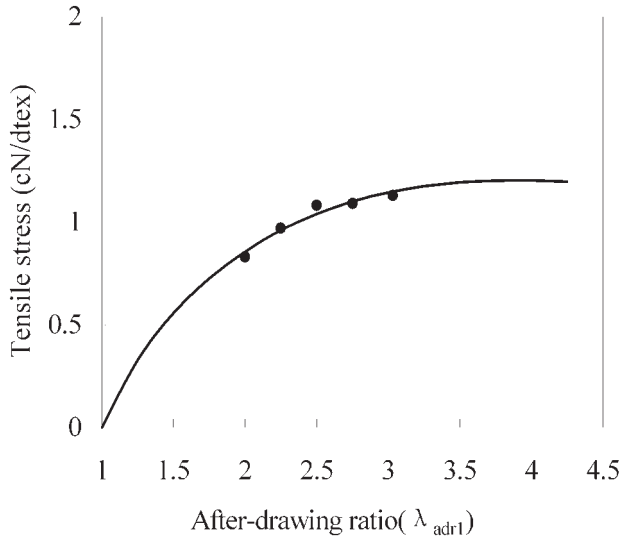

Figure 10 Tensile stress of the after-drawing (first step) versus the after-drawing ratio λ_{adr1} for $\bar{\lambda} = 2.51$; (●) experimental; (−) theoretical.

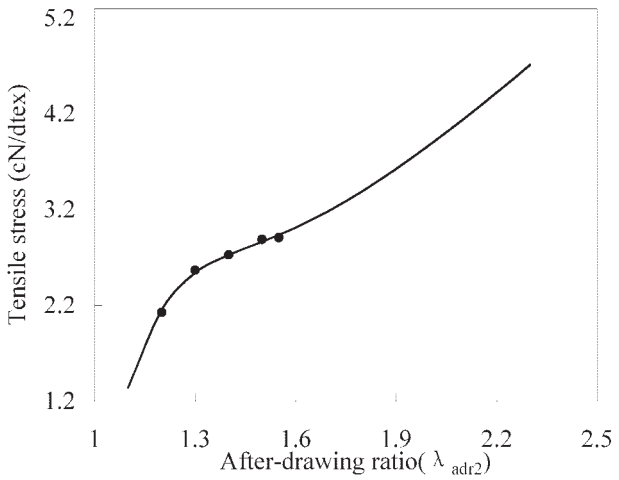

Figure 12 Tensile stress of the after-drawing (second step) versus the after-drawing ratio λ_{adr2} for $\bar{\lambda} = 1.39$; (●) experimental; (−) theoretical.

were all equal to zero, which indicated that, under the high temperature and drawing stress of the after-drawing process, no fixed agglomerate entanglements showed. The N_skT values of the first and second after-drawing of the experimental series 2 were all lower than that of the experimental series 1, and the two step after-drawing ratio of the experimental series 2 ($\lambda_{adr1} \times \lambda_{adr2} = 3.4 \times 1.31 = 4.45$) was higher than that of the experimental series 1 ($\lambda_{adr1} \times \lambda_{adr2} = 2.51 \times 1.39 = 3.49$). These results indicated that the lower feeding speed favored high ratio drawing and the macromolecular chain extension, corresponding to the lower number of network chains reflecting slippage agglomerate entanglements. The extensional viscosity η values of the first and second after-drawing of the experimental series 2 were all higher than that of the experimental series 1, which indicated that the viscous or internal friction extent between the chain segments of the relative molecular movement of the experimental series 2 was higher than that of the experimental series 1. This might be related to the higher molecular chain movement unit amount, length of the experimental series 2, and the shorter intermolecular distance (as for the second after-drawing of the experimental series 2). The entanglement numbers per macromolecule and the repeat unit —CH_2— numbers between entanglements for the after-drawing process are shown in Ta-

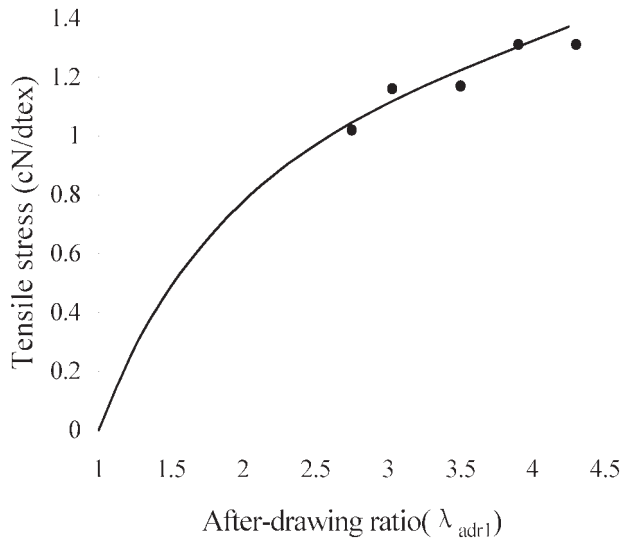

Figure 11 Tensile stress of the after-drawing (first step) versus the after-drawing ratio λ_{adr1} for $\bar{\lambda} = 3.4$; (●) experimental; (−) theoretical.

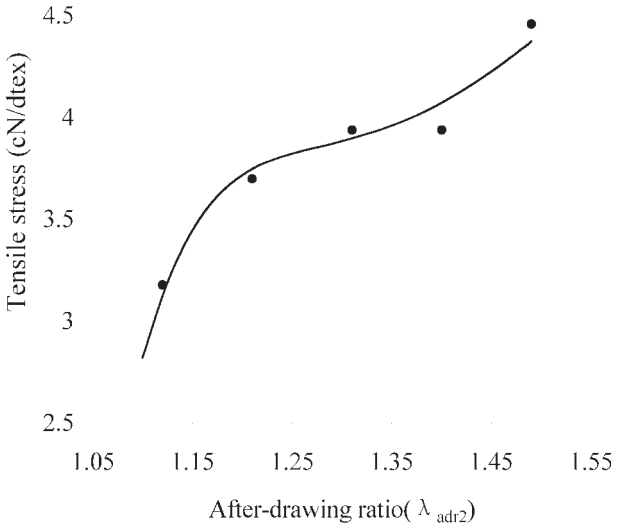

Figure 13 Tensile stress of the after-drawing (second step) versus the after-drawing ratio λ_{adr2} for $\bar{\lambda} = 1.31$; (●) experimental; (−) theoretical.

TABLE XI
The Fitted Parameters for the Molecular Entanglement Model of Entropy and Viscosity Composition for Different After-Drawing

	Parameter value			
	First step after-drawing		Second step after-drawing	
Parameter	$\bar{\lambda} = 0.013$ s^{-1}; $\bar{\dot{\varepsilon}} = 2.51$	$\bar{\lambda} = 0.010$ s^{-1}; $\bar{\dot{\varepsilon}} = 3.4$	$\bar{\lambda} = 0.009$ s^{-1}; $\bar{\dot{\varepsilon}} = 1.39$	$\bar{\lambda} = 0.005$ s^{-1}; $\bar{\dot{\varepsilon}} = 1.31$
α^2	0	0	0.41	0.36
β	0.03	0.06	0.55	0.46
N_ckT (MPa)	0	0	0	0
N_skT (MPa)	51.86	37.28	25	8.39
η (MPa s)	486.2	6270	13700	42900

$V_0 = 4$ m/min for $\bar{\lambda} = 2.51$, $V_0 = 2$ m/min for $\bar{\lambda} = 3.4$, $V_0 = 11$ m/min for $= 1.39$, $V_0 = 7.5$ m/min for $\bar{\lambda} = 1.31$; $L = 8$ m.

ble XII. It can be seen that the agglomerate entanglements have reached very high extent, and was related to the drawing stage and drawing conditions.

CONCLUSIONS

The entropy–viscosity model can set up the relationship between the macroscopic measurable quantity (drawing stress) and the microcosmic quantity (macromolecular entanglements). By the analytic results of the macromolecular slip entanglements, it is found that the N_skT value, which reflects the chain slippage at the macromolecular slip entanglements in the extensional deformation of the draw-down on the spinning line, increased to a maximum with the increase in the draw-down ratio, and after the peak value it decreased with further increase of the draw-down. This variation tendency is in accordance with the fact that each of the relationship curves between the tensile strength, modulus of the UHMWPE fibers (through maximized solid state drawing) and the draw-down ratio showed a peak, thus the molecular movement mechanism of "disentanglement on spinning line" in the dry spinning process of the UHMWPE/decalin solution is discovered. Based on this, the optimum draw-down ratio can be determined directly by measuring the draw-down stress at the exit of the spinning duct.

From the N_skT values obtained by combining the theoretical model with experimental data, it can be calculated that, in the experimental conditions of this research, the maximum value of the macromolecular slip entanglements was 14.58 when the UHMWPE/decalin spinning dope was extruded out of the spinning holes. The molecular entanglement number shown in the draw-down process on the spinning line might be related to the flow unit sizes of the macromolecular chains or macromolecular clusters. When the entanglements were included in the flow units, their apparent quantity would decrease.

The molecular entanglement numbers, which are obtained by theoretical fitting to the experimental data of the predrawing process in the dry spinning of the UHMWPE/decalin solution, increased dramatically. It can be concluded that these are mainly not attributed to the topological entanglements, but to the agglomerate entanglements. The agglomerate entanglements mainly showed as slip entanglements because of the weak interaction, and their quantity was apt to be affected by external conditions. Under suitable drawing temperature and extensional force, the relative slippage of the molecular chains in the crystalline region and the crystalline rearrangement would take place, which could behave as agglomerate entanglements.

The optimal processing temperature for each after-drawing stage was in accordance with the first melting endothermic peak temperature in the unconstrained DSC-thermogram of the corresponding processing stage fiber. From the results of the theoretical fitting to the experimental data of the after-drawing process, it was shown that the agglomerate entanglements reached a very high extent, and related to the drawing stage and drawing conditions. The molecular entanglements number of the full drawn UHMWPE fiber, estimated from the thermal shrinkage data according to Smook-Kalb method, was 5.28 and 6.21 respectively, (corresponding to the low and high feeding speed), which indicated that the solid state drawing condition could affect the molecular entanglements number in the end UHMWPE fiber calculated by this method.

Different from the results in the draw-down process on the spinning line (the results that the more the network chains reflecting the topological entanglements, the higher the "disentanglement on spinning line" and the end UHMWPE fiber performances), in the solid state drawing process the lower number of network chains (which reflect the agglomerate entanglements) was in favor of the increase of the macro-

TABLE XII
The Shown Entanglement Number per Macromolecule and the Repeat Unit Number Between the Entanglements During the After-Drawing Process, Calculated from the Fitted Parameters of the Molecular Entanglement Model of Entropy and Viscosity Composition

N_ckT (MPa)	0	0	0	0
Equivalently fixed links	0	0	0	0
N_skT (MPa)	51.86	37.28	25	8.39
Slip links	35114	25242	15864	5232
—CH_2— number between entanglements	4.27	5.94	9.23	28.0

molecular chain's extension, orientation and taut tie molecules, thus favorable to the preparation of high performance UHMWPE fiber.

References

1. Kavesh, S. Honeywell International WO 01/73173 A1. World Intellectual Property, 2001.
2. Sun, Y. China Petrochemical Company and China Textile Academy. CN Pat. 1,400,342A (2003).
3. Sun, Y.; Wang, Q.; Li, X. J Appl Polym Sci 2005, 98, 474.
4. Smook, J.; Pennings, J. Colloid Polym Sci 1984, 262, 712.
5. ASTM D-4020–01a.
6. Brereton, M. G.; Klein, P. G. Polymer 1988, 29, 970.
7. Edwards, S. F.; Vilgis, Th. Polymer 1986, 27, 483.
8. Thirion, T.; Weil, T. Polymer 1984, 25, 609.
9. Ball, R. C.; Doi, M.; Edwards, S. F. Polymer 1981, 22, 1010.
10. Kalb, B. J Mater Sci 1980, 15, 2584.
11. Xiao, C. Text J (China) 1997, 18, 11.
12. Shen, D.; Qian, R. Polym Bull (China) 1993, 4, 193.
13. Pang, W. Funct Polym J (China) 1999, 12, 49.